NUMERICAL IMPLEMENTATION OF MODELS FOR RADIATIVE PROPERTIES OF MOLECULAR GASES AND PARTICULATE MEDIA IN COMBUSTION APPLICATIONS

by

Lyubima Simeonova Nathan

A thesis submitted to the faculty of
The University of Utah
in partial fulfillment of the requirements for the degree of

Master of Science

Department of Chemical Engineering

The University of Utah

May 2012

The University of Utah Graduate School

STATEMENT OF THESIS APPROVAL

The thesis of **Lyubima Simeonova Nathan**

has been approved by the following supervisory committee members:

James Sutherland	, Chair	**03/07/2012** Date Approved
Philip Smith	, Member	**03/07/2012** Date Approved
Jeremy Thornock	, Member	**03/07/2012** Date Approved

and by **JoAnn Lighty**, Chair of the Department of **Chemical Engineering**

and by Charles A. Wight, Dean of The Graduate School.

ABSTRACT

Some of the most important engineering applications of thermal radiation are in the areas of combustion of gaseous, liquid, or solid fuel for power production or for propulsion. During combustion, thermal radiation will carry energy directly from the combustion products to the burner walls, often at rates higher than for convection. In the combustion process there are many intermediate reactions, intermittent generation of a variety of intermediate species, generation of soot, agglomeration of soot particles, and their subsequent partial burning. Any understanding and modelling of the combustion process requires knowledge of the radiation properties of the combustion gases and any particulates that are present. Models of these radiative properties will be reviewed in combustion applications. These models are implemented numerically. The convergence and accuracy of the algorithms and the challenges and solutions in increasing the efficiency of the developed software are discussed.

CONTENTS

LIST OF FIGURES

LIST OF TABLES

ACKNOWLEDGMENTS

I would like to thank my parents, Sofiya and Botyo, and my brother, Ivan, for their love, support, encouragement and the many sacrifices they have made, so I have the opportunities to pursue my goals and dreams. My family is my rock, and the paradigm of the person I hope to become.

I have been extremely fortunate in having terrific mentors. I am eternally indebted to my advisor Professor James Sutherland. I have benefited immensely from his help, encouragement, enthusiasm, and computational insight. I am deeply grateful to him for his many suggestions, helpful discussions, valuable advice, and for his careful reading and useful comments on many of the thesis drafts and the simulation code.

I am very grateful to Professors Philip Smith and Jeremy Thornock for their patience, wisdom, experience, and the privilege of working with them. I would like to thank them for the many valuable discussions and suggestions.

I have had many friends in the department who helped me through difficult times and shared the joy of my successes – Isaac, Matt, Brandon, Ben. Their friendship and support have made my graduate years happy and exciting.

Finally, I would like to thank the supportive staff of the Chemical Engineering Department for all their help and friendship.

CHAPTER 1

RADIATIVE TRANSFER EQUATION

The radiative transfer equation (RTE) is obtained by an energy balance on the radiative energy travelling in the direction $\widehat{s}$ within a small pencil of rays. The change in intensity is found by summing the contributions from emission, absorption, scattering away from the direction $\widehat{s}$, and into direction $\widehat{s}$:

$$\frac{1}{c}\frac{\partial I_\eta}{\partial t} + \frac{\partial I_\eta}{\partial s} = \kappa_\eta I_{b\eta} - \kappa_\eta I_\eta - \sigma_{s\eta} I_\eta + \frac{\sigma_{s\eta}}{4\pi}\int_{4\pi} I_\eta\left(\widehat{s}_i\right)\Phi_\eta\left(\widehat{s}_i,\widehat{s}\right)\, d\Omega_i, \tag{1.1}$$

where c is the speed of light, I_η is the spectral intensity, $I_{b\eta}$ is the spectral blackbody intensity, κ_η is the absorption coefficient, $\sigma_{s\eta}$ is the absorption coefficient. The function Φ_η is the scattering phase function. It describes that a ray from an incoming direction $\widehat{s}_i$ will be scattered into the direction $\widehat{s}$, and the integration is over all solid angles $d\Omega_i$ of incoming rays. All quantities may vary with location in space, time, and wavenumber, while the intensity and the phase function also depend on directions $\widehat{s}$ and $\widehat{s}_i$. In combustion applications, the speed of light is so large compared to local time and length scales that the first term in equation (1.1) may be neglected to obtain the quasi-static transfer equation.

$$\frac{\partial I_\eta}{\partial s} = \kappa_\eta I_{b\eta} - \kappa_\eta I_\eta - \sigma_{s\eta} I_\eta + \frac{\sigma_{s\eta}}{4\pi}\int_{4\pi} I_\eta\left(\widehat{s}_i\right)\Phi_\eta\left(\widehat{s}_i,\widehat{s}\right)\, d\Omega_i. \tag{1.2}$$

1.1 Heat Transfer

The spectral solutions of equation (1.2) are used to find the radiative heat flux, q_r. The spectral radiative heat flux onto a surface element has been expressed in terms of incident and outgoing intensity as

$$q_\eta \cdot \widehat{n} = \int_{4\pi} I_\eta \widehat{n}\cdot\widehat{s}\, d\Omega.$$

Removing the surface normal, the definition for the spectral radiative heat flux vector inside a participating medium is obtained. The total radiative heat flux is obtained by integrating over the whole spectrum

$$q_r = \int_0^\infty q_\eta \, d\eta = \int_0^\infty \int_{4\pi} I_\eta \left(\widehat{s}\right) \widehat{s} \, d\Omega \, d\eta.$$

The heat flux vector includes the radiative heat flux and is defined as

$$q = k_c \nabla T + q_r + \sum_j n_j h_j v_j + q_{d-1}.$$

The first term is the Fourier's law for heat conduction; the third term describes the heat transport by each of the diffusing species, where h_j is the partial molar enthalpy and v_j is the diffusion velocity of species j, and the fourth term is the heat transfer by the diffusion-thermo, or Dufour, effect and is related to a concentration driving force. In combustion problems modeling heat transfer in industrial furnaces the radiative heat flux dominates the heat transfer.

The divergence of the heat flux enters the overall conservation of energy equation

$$\frac{\partial \rho e}{\partial t} = -\nabla \cdot \rho e v - \nabla \cdot P v - \nabla \cdot q + S,$$

where ρ is the total mass, ρe is the energy density, v is the fluid velocity, P is pressure, and S is local volumetric heat source/sink. The divergence of the spectral radiative heat flux is given by

$$\nabla \cdot q_\eta = 4\pi \kappa_\eta I_{b\eta} - \left(\kappa_\eta + \sigma_{s\eta}\right) \int_{4\pi} I_\eta \left(\widehat{s}\right) \, d\Omega + \sigma_{s\eta} \int_{4\pi} I_\eta \left(\widehat{s}_i\right) \, d\Omega_i, \tag{1.3}$$

and the divergence of the total radiative heat flux $\nabla \cdot q_r$ is obtained by integrating equation (1.3) over the whole spectrum.

1.2 Numerical Implementation

ARCHES is a finite-volume large eddy simulation code developed by The Institute for Clean and Secure Energy at the University of Utah [1]. It incorporates predictive tools for highly turbulent, multiphase, reacting flows in industrial systems. The ARCHES component was initially designed for predicting the heat-flux from large buoyant pool fires with potential hazards immersed in or near a pool fire of transportation fuel. Since then, this component has been extended to solve many industrially relevant problems such as industrial flares, oxy-coal combustion processes, and fuel gasification.

The radiation transfer equation is solved in ARCHES according to the Discrete Ordinates Method. This numerical algorithm discretizes the entire solid angle ($\Omega = 4\pi$) using a finite number ordinate directions and corresponding weight factors. The RTE is written for each ordinate and the integral terms are replaced by a quadrature summed over each coordinate. The current models for predicting the radiative properties of gases are based on Hottel's charts that describe the absorption coefficients as functions of temperatures, pressure, and concentration of the gas. For this method, appropriate polynomials are curve-fitted for a given temperature and pressure (usually $1atm$). The method assumes uniform gas mixture and is not appropriate if scattering particles are present.

A Monte Carlo Ray Tracing algorithm that is parallelizable to thousands of processors is being developed at the institute to replace the current method in ARCHES [1]. In a Monte Carlo Ray Tracing approach, a finite number of photon histories is simulated through a random number generator. Each photon history is assigned initial energy, position, and direction. The number of free paths that the photon propagates is determined stochastically. The absorption and scattering coefficients of the media are sampled to determine if the collided photon is absorbed or scattered by the gas molecules and particles in the media. If scattered, the distribution of scattering angles is sampled and a new direction is assigned to the photon. If the scattering is elastic, a new energy is determined by the conservation of energy and momentum equations. The new RTE solver also requires better radiative properties methods that allow for non-uniform medium with clouds of particles to enhance accuracy of the computations.

CHAPTER 2

RADIATIVE PROPERTIES OF MOLECULAR GASES

A single spectral line at a certain spectral position is fully characterized by its strength (the intensity, or integrated absorption coefficient) and its line half-width. However, a vibration-rotation band may has many closely spaced spectral lines that may overlap considerably. While the absorption coefficient for individual lines may simply be added to give the absorption coefficient of an entire band at any spectral position,

$$\kappa_\eta = \sum_j \kappa_{\eta j},$$

the resulting function tends to gyrate violently across the band (as seen in Figure 2.1), unless the lines overlap very strongly. This tendency, plus the fact that there may be tens of thousands of spectral lines, makes radiative transfer calculations extremely difficult to carry out, if exact relationship is to be used in the spectral integration for total intensity, total radiative heat flux, or the divergence of the heat flux. The number of spectral lines for some of the radiative species in the HITRAN/HITEMP radiation databases [2] is displayed on Table 2.1. The enormous number of lines that must be considered, make line-by-line calculations, relying on detailed knowledge about the absorption coefficient for every spectral line, infeasible for combustion computations.

The temperature dependence comes from three contributions [3]:

1. from the partition function $Q(T)$
2. from the stimulated emission term, $\exp(-hc_0\eta/kT)$
3. from the lower energy state E_l.

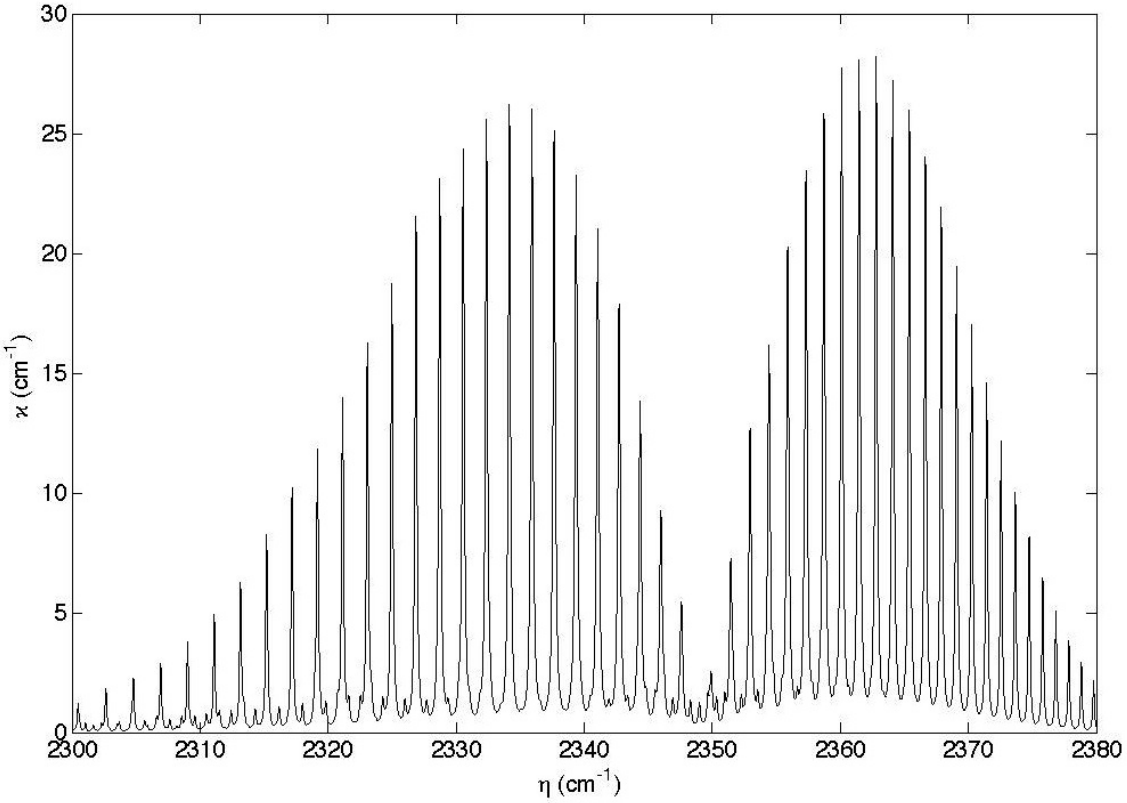

Figure 2.1. Spectral absorption coefficient, κ, for 10% of CO_2 in nitrogen; $4.3\mu m$ band at $p = 1.0$ bar, $T = 296$ K.

Table 2.1. Number of spectral lines for several radiative species typical in combustion applications.

Species	Spectral Lines
H_2O	114,241,164
CO_2	11,193,608
OH	105,366
CO	113,631
NO	115,610

The vibrational partition function can be determined, assuming a harmonic oscillator, as [4]

$$Q_v(T) = \prod_k \left(1 - e^{-hc_0\eta_k/kT}\right)^{-g_k},$$

where the product is over all the different vibrational modes with their harmonic oscillation wavenumbers $\eta_k = {}^{v_e}/_{c_0}$, and g_k is the degeneracy of the vibrational mode. The rotational partition function depends on the symmetry of the molecule and on the moments of inertia for rotation around two (linear molecule) or three (nonlinear molecule) axes. For moderate to high temperatures, i.e., when ${}^{2IkT}/_{h^2} \gg 1$ [4, 5],

- Linear molecules ($I_x = I_y = I$):

$$Q_r(T) = \frac{1}{\sigma}\frac{2IkT}{h^2} \propto T, \tag{2.1}$$

- Nonlinear molecules:

$$Q_r(T) = \frac{1}{\sigma}\prod_{i=x,y,z}\left(\frac{2I_ikT}{h^2}\right)^{1/2} \propto T^{3/2}, \tag{2.2}$$

where σ is a symmetry number, or the number of distinguishable rotational modes. Consideration of the separate contributions to the temperature dependence shows that, at moderate temperatures, the rotational partition function causes the line strength to decrease with temperature as ${}^1/_T$ or ${}^1/_{T^{3/2}}$, while the influences of the vibrational partition function and of induced emission are very minor (but may become important for $T > 1000K$) [3]. The influence of the lower energy state E_l can be negligible or dramatic, depending on the size of E_l: for small values of E_l (low vibration levels) $\exp({}^{-hc_0\eta}/_{kT}) \simeq 1$ and further raising the temperature will not change this value. On the other hand, large values of E_l (associated with high vibrational levels) make line strengths very small at low temperatures, but produce sharply increasing line strengths at elevated temperatures (when more molecules populate the higher vibrational levels), giving rise to so-called "hot lines" and "hot bands" [3].

The example in Figure 2.2 shows a small part of the spectrum of the $4.3\mu m$ CO_2 band generated from the HITRAN96 database [2]. At the high temperatures usually encountered during combustion the spectral lines narrow considerably, decreasing line overlap; at the same time the strengths of the lines that were most important at low temperature decrease according to equation (2.1) or equation (2.2) and finally, at high temperatures "hot lines," that were negligible at room temperature, become more and more important. The result is a fairly erratic looking absorption coefficient as depicted in the bottom frame of Figure 2.2.

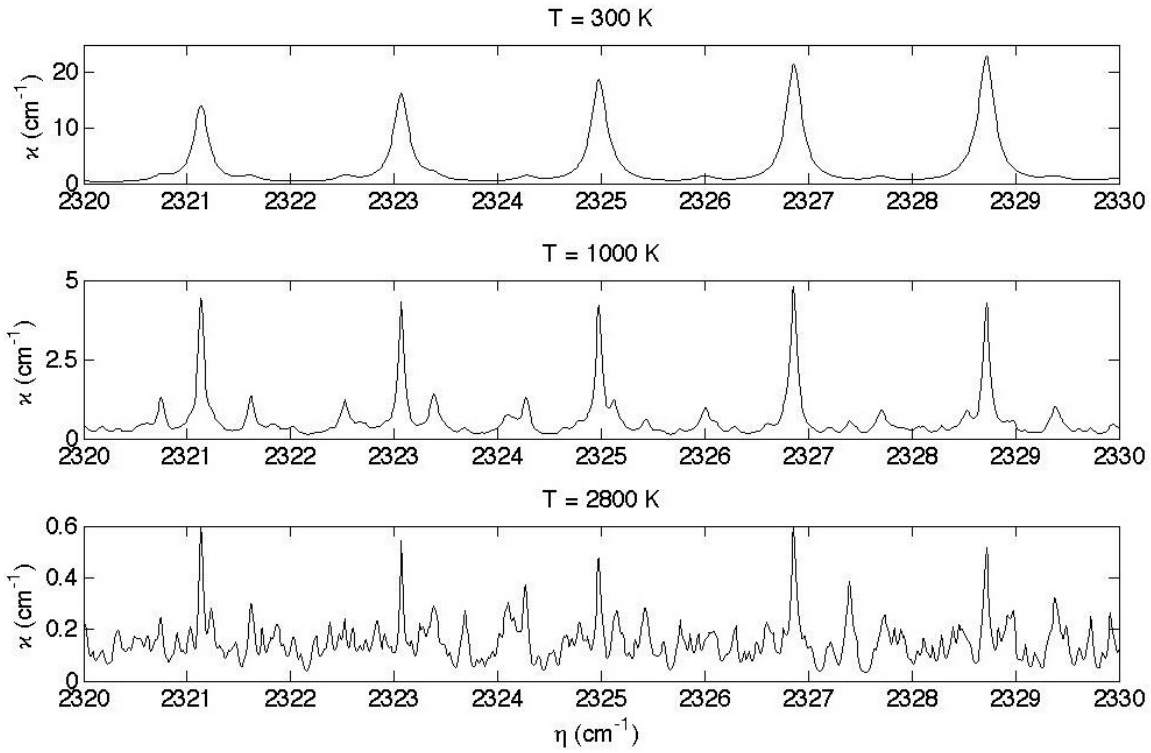

Figure 2.2. Spectral absorption coefficient for 10% of CO_2 in nitrogen, across a small portion of the CO_2 $4.3\mu m$ band at $p = 1.0$ bar; top frame: $T = 300K$; center frame: $T = 1000K$; bottom frame $T = 2800K$.

The absorption coefficient's dependence on the temperature is described by the relations (2.1) and (2.2), i.e., for linear molecules the absorption coefficient decreases proportionally to $1/T$ (Figure 2.3), and for nonlinear molecules - as $1/T^{3/2}$ (Figure 2.4).

Calculations involving the entire spectrum are a formidable task. The gas absorption coefficient varies wildly even across a very narrow spectrum, attaining the same value for the absorption coefficient many times, each time producing the identical intensity field within the medium. Thus, carrying out line-by-line calculations across such a spectrum would be rather wasteful, repeating the same calculation again and again. On the other hand, the Planck function remain essentially constant over a small spectral interval. This has prompted the development of a number of approximate spectral methods, of which the Full-Spectrum k-Distribution method seems most promising because it provides good accuracy and simplified integration of smooth functions of redefined variables instead of the highly oscillatory functions in the true variables, by reordering the absorption coefficients into a smooth monotonically increasing function.

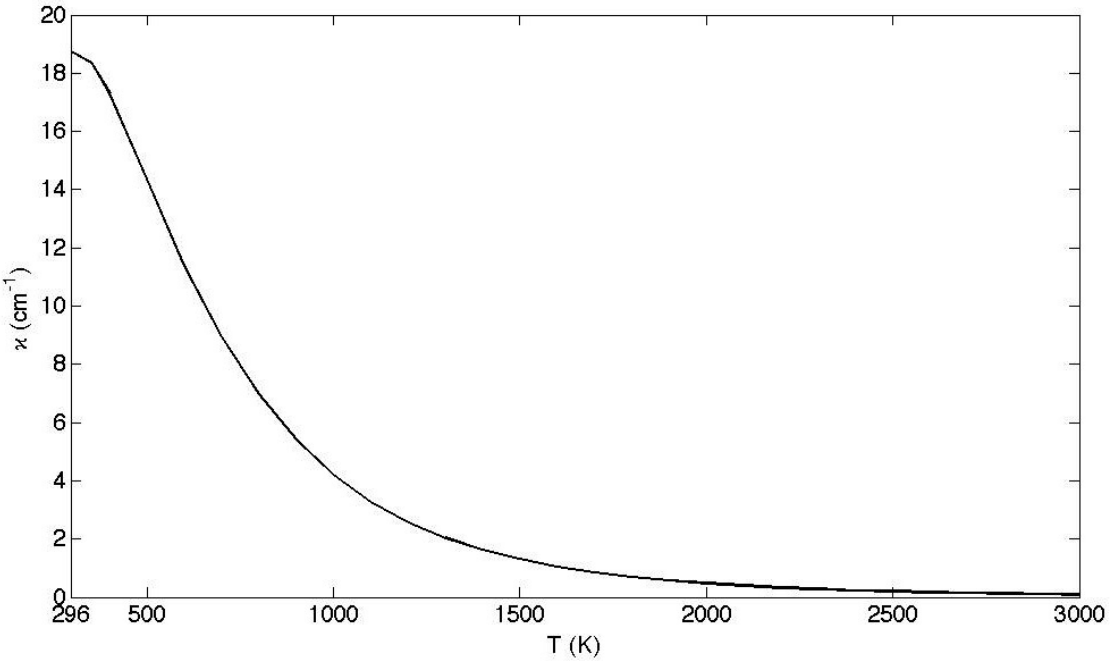

Figure 2.3. Spectral absorption coefficient for 10% CO_2 in nitrogen for wavenumber $\eta = 2324.98 cm^{-1}$.

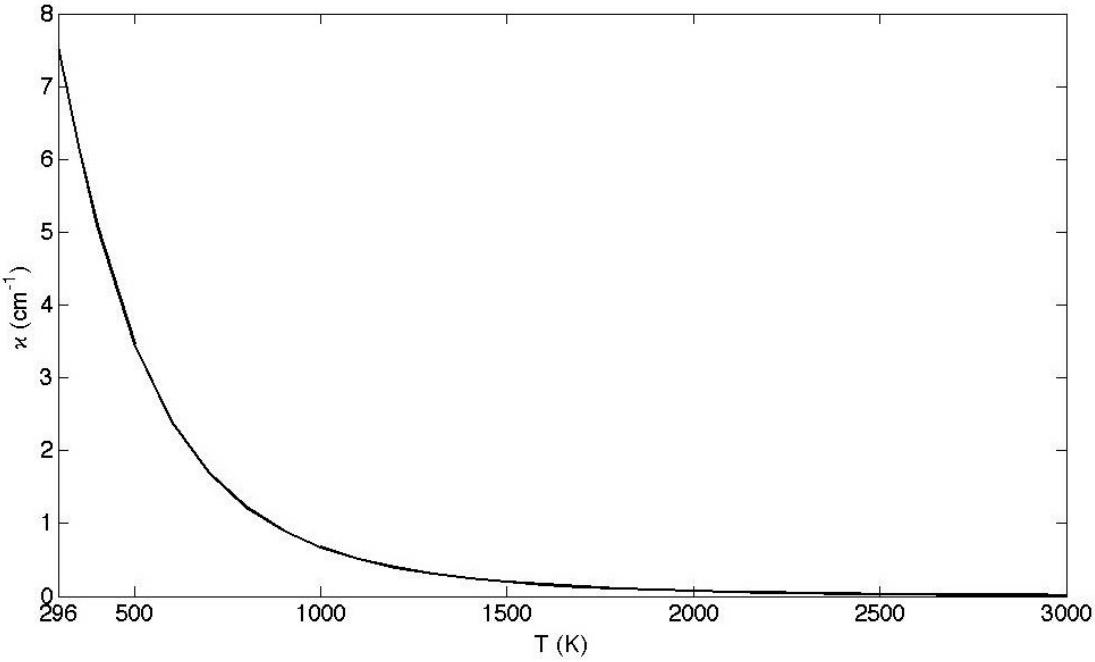

Figure 2.4. Spectral absorption coefficient for 10% H_2O in nitrogen for wavenumber $\eta = 202.70 cm^{-1}$.

2.1 Full Spectrum k-Distributions

Recent approaches to band correlations have led to helpful simplifications. Most of these methods involve transforming the spectral distribution of the absorption coefficient into a probability density versus absorption coefficient space for a given narrow or wide band, and in some cases integrating the probability density function (PDF) to give a cumulative distribution function (CDF) of the absorption coefficient. The smoothly varying PDF or CDF is then used to provide spectral property dependence in the radiative transfer relations. The PDFs and CDFs must be developed from fundamental data on the spectral line absorption behavior in each band from the HITRAN database for low temperatures, and in HITEMP for higher temperature data.

The Full-Spectrum k-Distribution (FSK) demands that, except for the absorption coefficient, no other radiative property varies across the spectrum, and then attempts to integrate the radiative transfer equation across the entire spectrum before solving it. This is achieved by reordering the absorption coefficient into a monotonically increasing function. In the full-spectrum case allowance must be made for the black body intensity (or Planck function) varying across the spectrum. This method has been proposed by Modest and Zhang [6]. The FSK method can also be applied directly to the RTE, resulting in a more powerful derivation, because it shows that the approach is also valid for arbitrary scattering media and for arbitrary reflecting surfaces, as long as the absorption coefficient remains the only spectrally varying radiative property[7, 8] .

2.1.1 The FSK Method for Homogeneous Media

The simple case of a homogeneous medium, i.e., a medium with uniform temperature, pressure, and mixture mole fraction throughout, is considered. Such a mixture has an absorption coefficient that, while varying across the spectrum, is spatially constant. The radiative transfer equation for such a medium is

$$\frac{dI_\eta}{ds} = \kappa_\eta I_{b\eta} - (\kappa_\eta + \sigma_s) I_\eta + \frac{\sigma_s}{4\pi} \int_{4\pi} I_\eta \left(\hat{\mathbf{s}}'\right) \Phi \left(\hat{\mathbf{s}}, \hat{\mathbf{s}}'\right) \, d\Omega', \tag{2.3}$$

where - in order to establish a global model - scattering coefficient and phase function are assumed to be independent of wavenumber (gray). Let equation (2.3) be subject to the boundary conditions at a wall

$$I_\eta = I_{w\eta} = \epsilon_w I_{bw\eta} - (1 - \epsilon_w) \frac{1}{\pi} \int_{\hat{\mathbf{n}} \cdot \hat{s} < 0} I_\eta \left| \hat{\mathbf{n}} \cdot \hat{\mathbf{s}} \right| \, d\Omega, \tag{2.4}$$

where $I_{w\eta}$ is the spectral intensity leaving the enclosure wall, due to (diffuse gray) emission and/or (diffuse gray) reflection (and extension to more general boundary conditions is straight forward provided the surface properties remain gray).

A full-spectrum k-distribution is defined as

$$f(T,k) = \frac{1}{I_b} \int_0^\infty I_{b\eta}(T)\delta(k-\kappa_\eta)\, d\eta. \tag{2.5}$$

The $f(T,k)$ in equation (2.5) is a Planck-function-weighted k-distribution and is a function of temperature through the black body intensity [3]. A reordered RTE is obtained by multiplying equations (2.3) and (2.4) by the Dirac-delta function $\delta(k-\kappa_\eta)$, followed by integration over the entire spectrum. This leads to

$$\frac{dI_k}{ds} = kf(T,k)I_b - (k+\sigma_s)I_k + \frac{\sigma_s}{4\pi}\int_{4\pi} I_k\left(\hat{\mathbf{s}}'\right)\Phi\left(\hat{\mathbf{s}},\hat{\mathbf{s}}'\right)\, d\Omega' \tag{2.6}$$

with boundary condition

$$I_k = I_{wk} = \epsilon_w f(T_w,k)I_{bw} - (1-\epsilon_w)\frac{1}{\pi}\int_{\hat{\mathbf{n}}\cdot\hat{s}<0} I_\eta\left|\hat{\mathbf{n}}\cdot\hat{\mathbf{s}}\right|\, d\Omega, \tag{2.7}$$

where

$$I_k = \int_0^\infty I_\eta(T)\delta(k-\kappa_\eta)\, d\eta \tag{2.8}$$

is the intensity I_η collected over all spectral locations where $k_\eta = k$ (per dk). Thus, once I_k has been found from equation (2.6), the total intensity can be determined from

$$I = \int_0^\infty I_{b\eta}\, d\eta = \int_0^\infty I_k\, dk. \tag{2.9}$$

Two Planck-function weighted k-distributions are required: one at the temperature of the homogeneous medium, $f(T,k)$, and one evaluated at the wall temperature, $f(T_w,k)$, but both evaluated at the absorption coefficient evaluated at the conditions of the medium [3]. The full-spectrum k-distributions span across many orders of magnitude, and may be quite ill-behaved. To facilitate integration of equation (2.8), equations (2.6) and (2.7) are divided by the k-distribution evaluated at the temperature of the medium. This leads to a reordered RTE in a smoothly-varying g-space, where the cumulative k-distribution g is a nondimensional, Planck-function-weighted, reordered wavenumber [3]. This is termed the Full-Spectrum k-Distribution (FSK) Method:

$$\frac{dI_g}{ds} = k\left(I_b(T) - I_g\right) - \sigma_s\left(I_g - \frac{1}{4\pi}\int_{4\pi} I_g\left(\hat{\mathbf{s}}'\right)\Phi\left(\hat{\mathbf{s}},\hat{\mathbf{s}}'\right)\,d\Omega'\right), \tag{2.10}$$

with the boundary conditions

$$I_g = I_{wg} = \epsilon_w a(T_w,T,g) I_{bw} - (1-\epsilon_w)\frac{1}{\pi}\int_{\hat{\mathbf{n}}\cdot\hat{s}<0} I_g\left|\hat{\mathbf{n}}\cdot\hat{\mathbf{s}}\right|\,d\Omega, \tag{2.11}$$

where

$$I_g = \frac{I_k}{f(T,k)} = \frac{\int_0^\infty I_\eta(T)\delta(k-\kappa_\eta)\,d\eta}{f(T,k)}, \tag{2.12}$$

$$g(T,k) = \int_0^k f(T,k)\,dk, \tag{2.13}$$

$$a(T_w,T,g) = \frac{f(T_w,k)}{f(T,k)} = \frac{dg_w(T_w,k)}{dg(T,k)}. \tag{2.14}$$

Physically, g is the Planck-function-weighted fraction of the spectrum with absorption coefficient $\kappa_\eta < k$. Thus, the total intensity is evaluated from

$$I = \int_0^\infty I_{b\eta}\,d\eta = \int_0^\infty I_k\,dk = \int_0^1 I_g\,dg. \tag{2.15}$$

In equation (2.14) the numerator and denominator are both evaluated at identical values of k, which in turn is related to g through equation (2.13) [3]. The function a is the stretching factor dg_w/dg between the two distributions. Wherever the slope of $k(T_w,g_w)$ is less than that of $k(T,g)$, $a(T_w,T,g) > 1$ and vice versa.

The FSK method given by equations (2.10) through (2.14) is an exact method (subject to the restriction of a homogeneous medium). In fact, the method is also exact for nonhomogeneous media, provided that the absorption coefficient is spatially invariant (e.g., evaluated at a reference condition and then applied to the entire medium) [3]. Within these restrictions the FSK results are equivalent to line-by-line calculations, the former requiring roughly ten spectral evaluations versus about one million for the line-by-line method.

The Planck function weighted cumulative k-distributions for 10% CO_2 in nitrogen for Planck function temperatures of 1000 K and 500 K are displayed in Figure 2.5. These are smooth, monotonically increasing functions of non-dimensional "wavenumber" g.

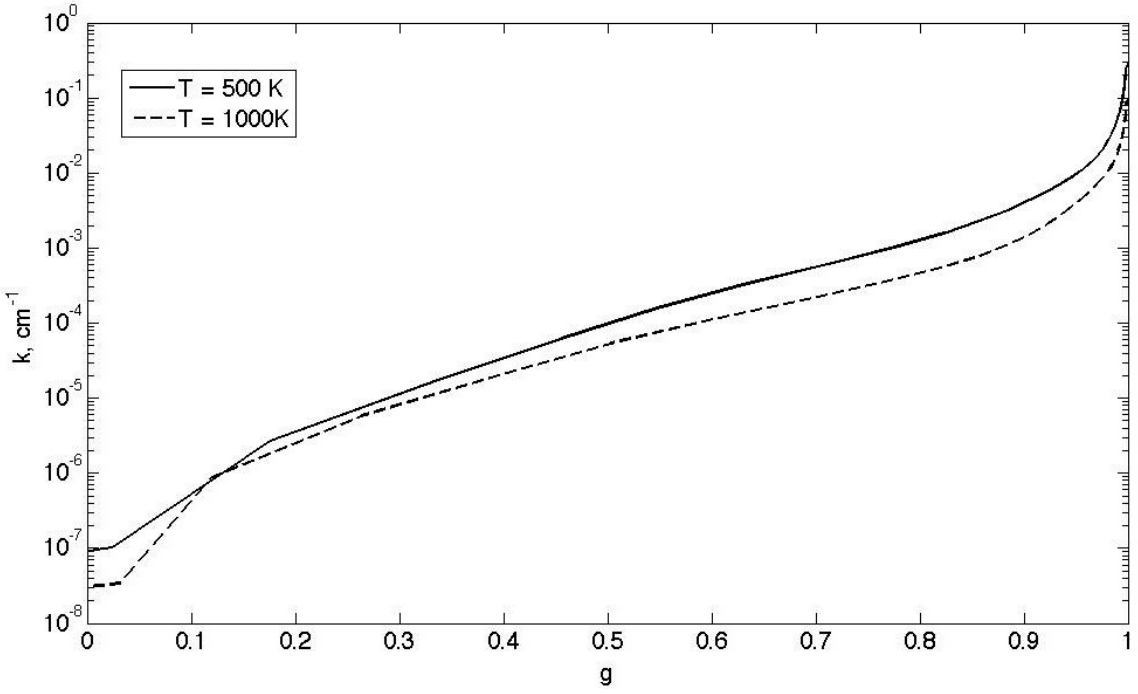

Figure 2.5. Planck function weighted cumulative k-distributions for 10% CO_2 in nitrogen for temperatures of 1000 K and 500 K.

2.1.2 Evaluation of k-Distributions

The reordering scheme requires that the values of k are grouped over small ranges $k_j \leq k < k_{j+1}$. Thus,

$$f(T, k_j)\delta k_j \backsimeq \sum_i \frac{I_{b\eta i}(T)}{I_b(T)} \left| \frac{\delta\eta}{\delta k_\eta} \right|_i \left[H\left(k_{j+1} - k_\eta\right) - H\left(k_j - k_\eta\right) \right], \tag{2.16}$$

where $H(k)$ is the Heaviside's unit step function,

$$H(x) = \begin{cases} 0, & x < 0, \\ 1, & x > 0, \end{cases}$$

and the summation over i collects all the occurrences where $k_j \leq k < k_{j+1}$. The absorption coefficient is known from the line-by-line data, and the k-distribution is calculated from equation (2.16). The total spectrum is broken up into N equal subintervals $\delta\eta$, the absorption coefficient k_η is evaluated at the center of each interval, and, if $k_j \leq k < k_{j+1}$, the value of each $f(T, k_j)\delta k_j$ is incremented by $\delta i(T) = {}^{I_{b\eta}(T,\eta_i)\delta\eta}/_{I_b(T)}$. The cumulative function $g(T, k)$ is calculated from the following equation

$$g(T, k_{j+1}) = \sum_{j'=1}^{j} f(T, k_{j'})\delta k_{j'} = g(k_j) + f(T, k_j)\delta k_j. \tag{2.17}$$

2.1.3 Treatment of Gas Mixtures

In principle, variable mixtures of different absorbing gases, and perhaps the addition of nonscattering particles, such as soot, pose no additional difficulty, because the absorption coefficient of all species can simply be added up. In practice, however, because of the considerable effort involved, it is preferable to precalculate and database all necessary k-distributions, before embarking on detailed heat transfer calculations. Because of the infinite number of possible mixture concentrations this would quickly become an enormous task. Therefore, is highly desirable to build k-distributions for arbitrary gas mixture from relatively few distributions databased for individual species. Exact construction of such k-distributions is possible as long as the absorption coefficient of each species is unaffected by the other species. This is not always the case, and a number of approximate mixing schemes are developed by Webb and collaborators [9, 7]. For applications to combustion, the random-overlap model is the most appropriate because it allows for overlap of the absorption coefficients of the different species across the spectrum. In order to implement this method, the k-distribution for a single absorbing species of varying concentration must be obtained.

2.1.3.1 A Single Absorbing Gas

Consider a gas whose absorption coefficient is linearly dependent on its partial pressure, i.e., a gas whose line broadening is unaffected by its own partial pressure. This is always true for molecules that have the same size as the surrounding broadening gas [3]. Then

$$\kappa_{x\eta}(x, T, p, \eta) = x\kappa_\eta(T, p, \eta), \tag{2.18}$$

where κ_η is the absorption coefficient of the pure gas and x is its mole fraction in a mixture. Comparing the two k-distributions

$$f(T, p; k) = \frac{1}{I_b}\int_0^\infty I_{b\eta}(T)\delta(k - \kappa_\eta)\, d\eta,$$

$$f(T, p; k_x = xk) = \frac{1}{I_b}\int_0^\infty I_{b\eta}(T)\delta(k_x - \kappa_{x\eta})\, d\eta,$$

it is seen that they are both populated by the same spectral locations, i.e. $k_x = \kappa_{x\eta}$ wherever $k = \kappa_\eta$, so that

$$f(T,p,x;xk)d(xk) = f(T,p;k)dk$$

or

$$f(T,p,x;xk) = \frac{1}{x} f(T,p;k) \tag{2.19}$$

This implies that the weight function a remains unaffected if the mole fraction is changed. Integrating equation (2.19) leads to

$$g(T,p,x;k) = \int_0^k f(T,p;k)\,dk = \int_0^{k_x} f(T,p,x;k_x)\,dk_x = g(T,p,x;k_x),$$

i.e., the k versus g behavior is independent of mole fraction. In a k versus g plot, the curves are simply vertically displaced by a factor of x.

2.1.3.2 k-Distributions for Random Overlap

As pointed out by Taine and Soufiani [10], there is no physical reason why there should be any significant correlation between the spectral variations of absorption coefficients of different gas species. The absorption coefficients are statistically independent random variables, and k-distributions are statistically uncorrelated. When considering the entire spectrum, the cumulative k-distributions of M species are multiplicative,

$$g(T,p;k) = g_1(T,p;k) \times g_2(T,p;k) \times \ldots = \prod_{m=1}^{M} g_m(T,p;k). \tag{2.20}$$

2.2 Mean Absorption Coefficients

A mean absorption coefficient that is spectrally averaged over all wavenumbers has been used as a simplification to approximate the correct procedure of carrying out a spectral analysis and then integrating the spectral energy over all wavenumbers to obtain the total energy.

2.2.1 Planck Mean Absorption Coefficient

The emission term in the equation of transfer and in the divergence of the radiative heat flux is proportional to $\kappa_\eta I_{b\eta}$. Thus, for the evaluation of total intensity or heat flux divergence it is convenient to define the following total absorption coefficient, known as the Planck mean absorption coefficient:

$$\kappa_P \equiv \frac{\int_0^\infty \kappa_\eta I_{b\eta}\, d\eta}{\int_0^\infty I_{b\eta}\, d\eta} = \frac{\pi}{\sigma T^4} \int_0^\infty \kappa_\eta I_{b\eta}\, d\eta. \tag{2.21}$$

Planck mean absorption coefficients for carbon dioxide and water vapor are displayed in Figure 2.6.

The Planck mean absorption coefficient is valid for the optically thin limit when radiation passes through the optically thin layer without much attenuation. The Planck mean absorption coefficient is calculated and tabulated for each species at different temperatures and weighted by the mole fraction of each species to calculate the Planck mean absorption coefficient for a gas mixture.

2.2.2 Rosseland Mean Absorption Coefficient

The Rosseland mean absorption coefficient is valid for the optically thick limit when the radiation that passes through the optically thick layer is highly attenuated. The radiative heat flux becomes proportional to

$$\frac{1}{\kappa_\eta} \nabla I_{b\eta} = \frac{1}{\kappa_\eta} \frac{dI_{b\eta}}{dT} \nabla T.$$

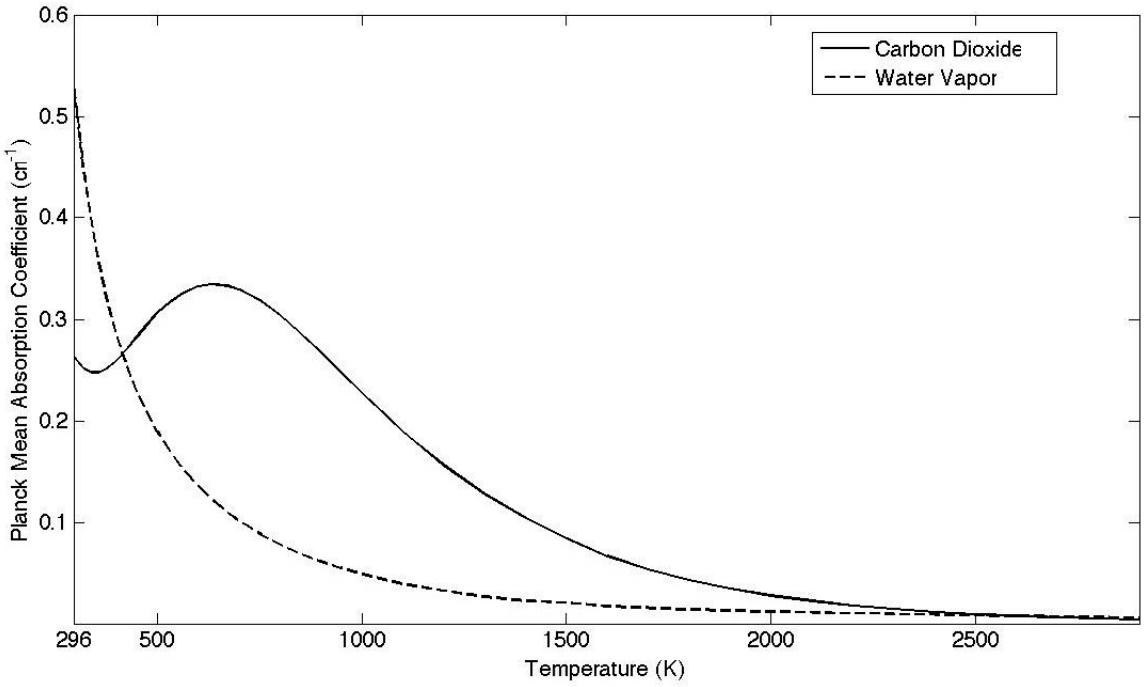

Figure 2.6. Planck mean absorption coefficient for carbon dioxide (solid line) and water vapor (dashed line).

This leads to the definition of an optically thick or Rosseland mean absorption coefficient as

$$\frac{1}{\kappa_R} \equiv \frac{\int_0^\infty \frac{1}{\kappa_\eta}\frac{dI_{b\eta}}{dT}\,d\eta}{\int_0^\infty \frac{dI_{b\eta}}{dT}\,d\eta} = \frac{\pi}{4\sigma T^3}\int_0^\infty \frac{1}{\kappa_\eta}\frac{dI_{b\eta}}{dT}\,d\eta. \tag{2.22}$$

The Rosseland mean absorption coefficient may not be appropriate for pure gases [3]. It is more appropriate for an optically thick particle background with or without molecular gases. In order to be combined with the absorption coefficient of a particulate cloud, the Rosseland mean absorption coefficient is calculated at different temperatures and tabulated.

2.2.3 Effective Mean Absorption Coefficient

The Effective mean absorption coefficient is a function of not only temperature and pressure, but also path length, L [11]. It is defined as

$$\kappa_E(L,T,P) \equiv \frac{\int_0^\infty \kappa_\eta I_{b\eta} e^{-\kappa_\eta S}\,d\eta}{\int_0^\infty I_{b\eta} e^{-\kappa_\eta S}\,d\eta}. \tag{2.23}$$

The values of κ_E are tabulated as a function of temperature and path length L. For small path length L, κ_E approaches the Planck mean absorption coefficient, κ_P. For large path length L, the exponential term in the integral causes κ_E to approach the minimum value of κ_η in the spectrum considered.

2.3 Numerical Algorithm

2.3.1 The Full-Spectrum k-Distribution Method

Files for the absorption coefficients of five radiative species, that participate in combustion, are accumulated at different temperatures from the HITRAN and HITEMP database [12]. The k-distributions for every species is calculated at a discrete set of temperatures in a pre-processing step. The files with the spectral information, containing the wavenumbers and the corresponding absorption coefficient, are loaded automatically by the constructor of the FSK class; the k-distributions are computed for each species and written in a text file in a pre-processing step. A second constructor loads the k-distribution file containing the species, temperatures, the g-values and the corresponding k-values for each temperature and species. The structure of the algorithm is displayed in Figure 2.7.

The k-distribution of the mixture is computed according to equation (2.20) from the k-distributions of the individual species. The absorption coefficient range is spaced logarithmically to better resolve the g-values for ranges with higher absorption coefficients that impact the accuracy of the radiative transfer equations solutions significantly.

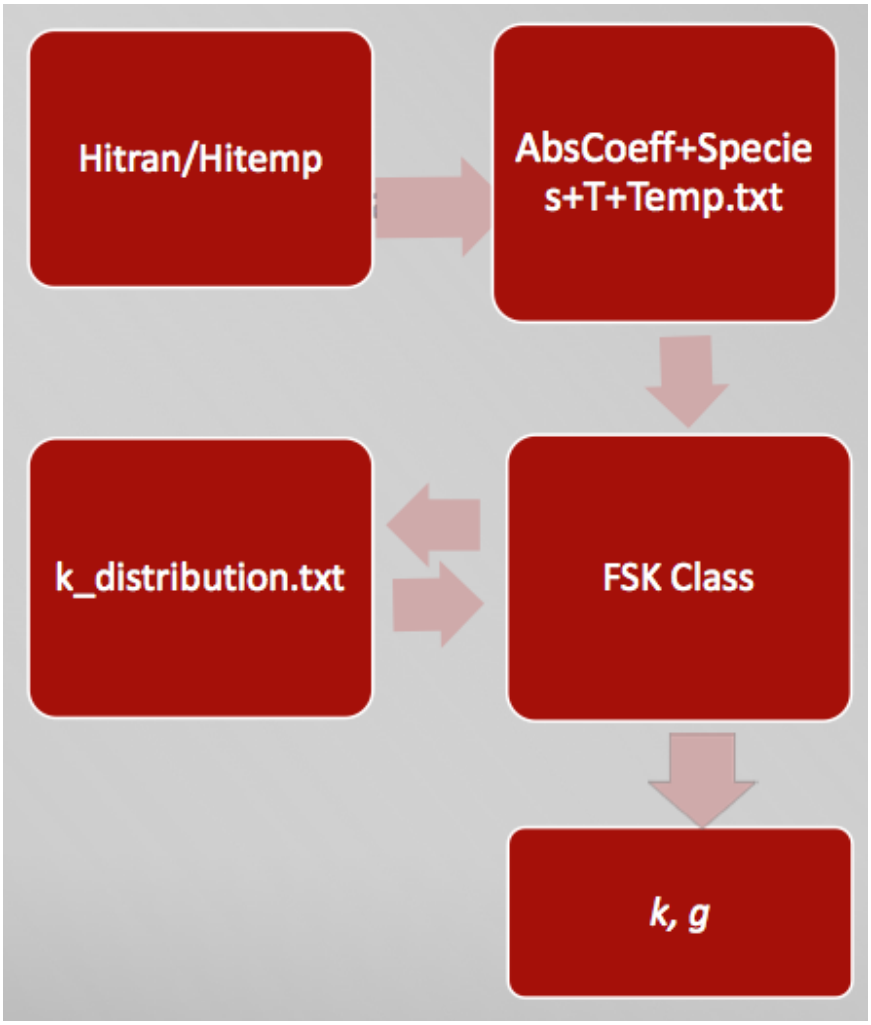

Figure 2.7. FSK algorithm structure.

The calculations of the mixture k-distributions in combustion simulations must be performed repeatedly to account for the variability in the composition and the temperature of the gases in combustion.

In order to decrease computation time, the dependence of the accuracy of the k-distribution on the number of g-values we compute is explored in Figure 2.8. Decreasing the number of g-values computed decreases the accuracy of the k-distribution only for small values of the absorption coefficient that have minimal effect on the radiative transfer computations, and they can be ignored in the calculation. The radiative transfer equation is solved for a discrete number of g-values, and the solutions are added according to equation (2.15) to compute the total intensity.

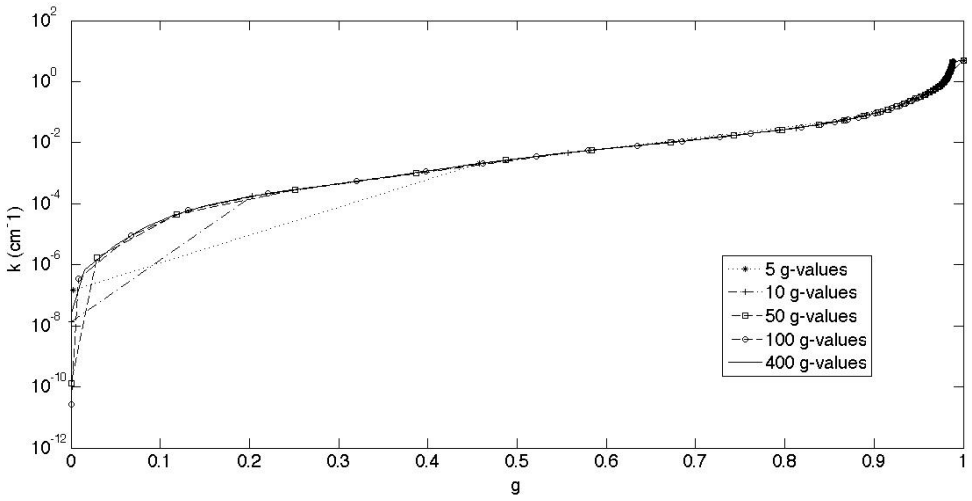

Figure 2.8. The dependence of the k-distribution approximation on the number of g-values for a mixture of 20% H_2O, 40% CO_2 , 5% CO, 0.3% NO, 5% OH at T = 1050 K.

Solutions to the radiative transfer equation are computationally expensive and decreasing the number of these computations while preserving accuracy can be accomplished using the full-spectrum k-distribution method with logarithmic spacing of the g-values.

A public method computes the k-distribution for the mixture from the k-distributions of each individual species according to equation (2.20) and interpolates linearly in temperature. Another public method computes the a-function participating in the wall-boundary condition according to equation (2.14).

2.3.2 Grey Gas Methods

Files for the absorption coefficients of five radiative species, that participate in combustion, are accumulated at different temperatures from the HITRAN and HITEMP database [12]. The Planck, Rosseland, and Effective mean absorption coefficients for every species are calculated at a discrete set of temperatures in a pre-processing step. The temperatures are spaced logarithmically to capture and better approximate the greater variability of the mean coefficients for small temperatures (Figure 2.6). The files with the spectral information, containing the wavenumbers and the corresponding absorption coefficient, are loaded automatically by the constructor of the Grey Gas class; the Planck, Rosseland, and Effective mean absorption coefficients for every species at each temperature are computed for each species and written in a text file in a pre-processing step. A second constructor loads

this file that contains the species, temperatures, and the mean coefficients. The structure of the algorithm is similar to that for the FSK method displayed in Figure 2.7.

The Planck, Rosseland, and Effective mean absorption coefficients of the mixture are computed by multiplying the coefficients of the individual species by the mole fractions and summing them, and linearly interpolating them in temperature. For 45 logarithmically spaced temperatures in the range $296K - 3000K$, the interpolation error is estimated to be $\frac{|k_{interp}-k|}{k} \leq 1e^{-3}$. The dependence of this error on the number of temperatures considered is displayed on Table 2.2.

The calculations of the mixture k-distributions in combustion simulations must be performed repeatedly to account for the variability in the composition and the temperature of the gases in combustion.

Table 2.2. Interpolation error dependence on number of temperatures considered.

N_T	10	20	45
ϵ	$2e^{-2}$	$3e^{-3}$	$1e^{-3}$

CHAPTER 3

RADIATIVE PROPERTIES OF PARTICULATE MEDIA

When an electromagnetic wave or a photon interacts with a medium containing small particles, the radiative intensity may be changed by absorption and scattering. How much and into which direction a particle scatters an electromagnetic wave passing through its vicinity depends on

1. the shape of the particle;
2. the material of the particle, i.e. the complex index of refraction, $m = n - ik$;
3. its relative size;
4. the clearance between particles.

In radiative analyses the shape of the particle is usually assumed to be spherical (for spherical and irregularly shaped objects) or cylindrical (for long fibrous materials). These simplifying assumptions give generally excellent results, since averaging over many millions of irregular shapes tends to smoothen the irregularities [13].

An electromagnetic wave or photon passing through the immediate vicinity of spherical particles will be absorbed or scattered. The scattering is due to three separate phenomena [3], namely,

1. diffraction (waves never come into contact with the particle, but their direction of propagation is altered by the presence of the particle);
2. reflection by a particle (waves reflected from the surface of the sphere);
3. refraction in a particle (waves that penetrate into the sphere and, after partial absorption, reemerge traveling into a different direction).

The vast majority of photons are scattered elastically, i.e., their wavelength (and energy) remains unchanged. A tiny fraction undergo inelastic or Raman scattering (the photons reemerge with a different wavelength). The Raman effect is unimportant for the evaluation of radiative heat transfer rates, and only elastic scattering effects are considered. If scattering by one particle is not affected by the presence of surrounding particles, the scattering is called independent; otherwise the scattering is called dependent. Thus, the radiative properties of a cloud of spherical particles of radius a, interacting with an electromagnetic wave of wavelength λ, are governed by three independent nondimensional parameters:

- complex index of refraction: $m = n - ik$;
- size parameter: $x = 2\pi a/\lambda$;
- clearance-to-wave ratio: c/λ, where c is the speed of light.

If scattering is independent ($c/\lambda \gg 1$), then only the first two parameters are needed. For the classification of dependent scattering, the clearance-to-wavelength ratio is often replaced by a purely geometric parameter, c/a, which in turn is related to the volume fraction of particles, f_v. While in earlier works, for example that by van de Hulst [14], it was assumed that dependent effects were a function of particle separation only, it is now known that wavelength effects are significant. This was first recognized by Hottel et al. [15]. Since then, a number of investigators, notably Tien and collaborators [16, 17, 18, 13, 19], have established limits for when dependent effects must be considered. Dependent scattering effects may be ignored as long as $f_v < 0.006$ or $c/\lambda > 0.5$. These values include nearly all heat transfer applications.

3.1 Radiation from a Single Sphere

The scattering and absorption of radiation by single spheres was first discussed during the later part of the 19th century by Lord Rayleigh, who obtained the simple solution for spheres whose diameters are much smaller than the wavelength of radiation (small size parameter $x \ll 1$). In 1908 Gustav Mie developed a solution to Maxwell equations for an electromagnetic wave train traveling through a medium with an imbedded sphere. The Mie scattering theory must be used if the size of the sphere is such that it is too large to apply Rayleigh theory, but too small to employ geometric optics (which requires $x \gg 1$ as well as $kx \gg 1$) [3].

Radiation interacting with a spherical particle may be scattered away from its original direction by an angle Θ, i.e., the propagation vector of the electric and magnetic fields may

be redirected by the scattering angle. The intensity of the wave scattered by the angle Θ is proportional to two complex amplitude functions $S_1(\Theta)$ and $S_2(\Theta)$, where the subscripts denote two perpendicular polarizations. Once these scattering amplitude functions have been determined, the intensity of radiation I_{sca}, scattered by an angle Θ from the incident unpolorized beam of strength I_{in} may be calculated [3] from

$$\frac{I_{sca}(\Theta)}{I_{in}} = \frac{1}{2}\frac{|S_1|^2 + |S_2|^2}{x^2}. \tag{3.1}$$

From equation (3.1) it follows that the total amount of energy scattered by one sphere into all directions is

$$Q_{sca} = \frac{1}{x^2}\int_0^{\pi} \left(|S_1|^2 + |S_2|^2\right) \sin(\Theta)\, d\Theta, \tag{3.2}$$

where Q_{sca} is called the scattering efficiency factor.

The total extinction, Q_{ext}, by a single particle (absorption within the particle, plus scattering into all directions) is related to the real part of the amplitude functions by

$$Q_{ext} = \frac{4}{x^2} Re\left\{S(0)\right\}, \tag{3.3}$$

where the amplitude function S is without a subscript because $S_1(0) = S_2(0)$ [3].

The major difficulty in the evaluation of scattering properties lies in the calculation of the complex amplitude functions $S_1(\Theta)$ and $S_2(\Theta)$. For the general case of arbitrary values for the complex index of refraction m and the size parameter x, the full Mie equations must be employed [3],

$$S_1(\Theta) = \sum_{n=1}^{\infty} \frac{2n+1}{n(n+1)} \left[a_n \pi_n(\cos(\Theta)) + b_n \tau_n(\cos(\Theta))\right], \tag{3.4}$$

$$S_2(\Theta) = \sum_{n=1}^{\infty} \frac{2n+1}{n(n+1)} \left[b_n \pi_n(\cos(\Theta)) + a_n \tau_n(\cos(\Theta))\right], \tag{3.5}$$

where the direction dependent functions π_n and τ_n are related to Legendre polynomials P_n by [3]

$$\pi_n(\cos(\Theta)) = \frac{dP_n(\cos(\Theta))}{d\cos(\Theta)},$$

$$\tau_n(\cos(\Theta)) = \cos(\Theta)\pi_n\left(\cos(\Theta)\right) - \sin^2(\Theta)\frac{d\pi_n(\cos(\Theta))}{d\cos(\Theta)},$$

and the Mie scattering coefficients a_n and b_n are complex functions of x and $y = mx$,

$$a_n = \frac{\psi_n'(y)\psi_n(x) - m\psi_n(y)\psi_n'(x)}{\psi_n'(y)\zeta_n(x) - m\psi_n(y)\zeta_n'(x)},$$

$$b_n = \frac{m\psi_n'(y)\psi_n(x) - \psi_n(y)\psi_n'(x)}{m\psi_n'(y)\zeta_n(x) - \psi_n(y)\zeta_n'(x)}.$$

The functions ψ_n and ζ_n are known as Riccati-Bessel functions.

Using the fact that - similarly to Legendre polynomials - the functions π_n and τ_n constitute sets of orthogonal functions leads to [3]

$$Q_{sca} = \frac{2}{x^2}\sum_{n=1}^{\infty}(2n+1)\left[|a_n|^2 + |b_n|^2\right],$$

$$Q_{ext} = \frac{2}{x^2}\sum_{n=1}^{\infty}(2n+1)Re\left\{a_n + b_n\right\}.$$

Thus, the absorption efficiency factor, Q_{abs}, is found [3]

$$Q_{abs} = Q_{ext} - Q_{sca}. \tag{3.6}$$

The spectral absorption and scattering efficiencies for a $0.1\mu m$ radius coal particle (refractive index of $2 - 0.6i$) are displayed on Figure 3.1.

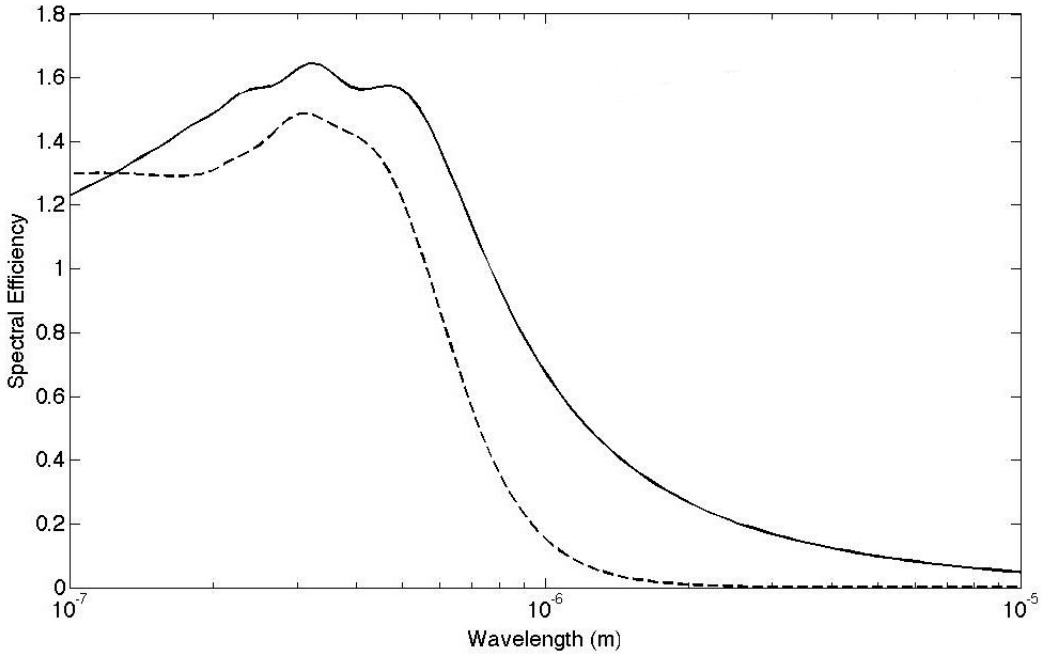

Figure 3.1. Spectral absorption (solid line) and scattering (dashed line) efficiencies for a $0.1\mu m$ radius coal particle.

3.2 Radiation of a Particle Cloud

In all problems of radiative heat transfer with particulate scattering and absorption, a large collection of particles must be considered. If the scattering is independent, as is the case for combustion processes, then the effects of large numbers of particles is additive. First, the case of particle clouds consisting of spheres that are all equally large is explained. The case that takes into account that particles of many different sizes may occur within a single cloud, is described.

3.2.1 Clouds of Uniform Size Particles

The fraction of energy scattered by all particles by unit length along the direction of the incoming beam is called the scattering coefficient. If N_T is the number of particles per unit volume, all of uniform radius a, then [3]

$$\sigma_{s\lambda} = \pi a^2 N_T Q_{sca}, \tag{3.7}$$

and, similarly, for absorption and extinction coefficients,

$$\kappa_\lambda = \pi a^2 N_T Q_{abs}, \tag{3.8}$$

$$\beta_\lambda = \pi a^2 N_T Q_{ext}. \tag{3.9}$$

Planck and Rosseland mean efficiencies are averaged values that represent the thin and thick gas limits, respectively, of the absorption and scattering efficiencies. They are commonly used in engineering applications to find the weighted means for variables which are wavelength dependent. The Planck and Rosseland mean efficiencies may be defined, respectively, as [20]

$$\bar{Q_P} = \frac{\int_0^\infty Q_\lambda I_{b\lambda}(T)\, d\lambda}{\int_0^\infty I_{b\lambda}(T)\, d\lambda} \tag{3.10}$$

and

$$\frac{1}{\bar{Q_R}} = \frac{\int_0^\infty \frac{1}{Q_\lambda}\frac{dI_{b\lambda}(T)}{dT}\, d\lambda}{\int_0^\infty \frac{dI_{b\lambda}(T)}{dT}\, d\lambda}. \tag{3.11}$$

Planck's spectral blackbody distribution can be substituted for the blackbody intensity and the resulting expressions integrated to give

$$\bar{Q_P} = \frac{15}{\pi^4}\int_0^\infty Q_\lambda \xi^3 (e^\xi - 1)^{-1}\, d\xi \tag{3.12}$$

and

$$\frac{1}{\bar{Q}_R} = \frac{15}{\pi^4} \int_0^\infty \frac{1}{Q_\lambda} \xi^4 e^\xi (e^\xi - 1)^{-2} \, d\xi \tag{3.13}$$

where $\xi = C_2/\lambda T$ can be thought of as a dimensionless frequency and $C_2 = 0.0144mK$ is Planck's second radiation constant.

The Planck and Rosseland mean absorption and scattering efficiencies for coal particles (refractive index of $2-0.6i$) of different radii are displayed in Figures 3.2 and 3.3, respectively.

The Planck and Rosseland mean absorption and scattering efficiencies for a coal particle (refractive index of $2 - 0.6i$) at different temperatures are displayed in Figures 3.4 and 3.5, respectively.

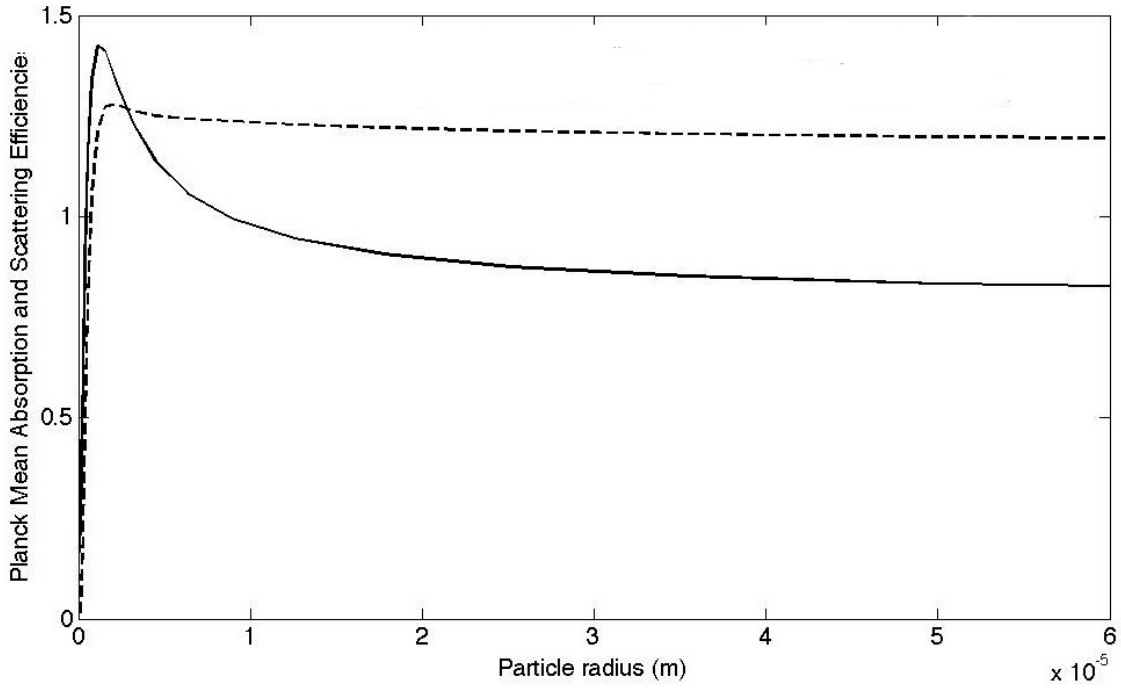

Figure 3.2. Variation of Planck mean absorption (solid line) and scattering (dashed line) efficiencies with coal particle radius.

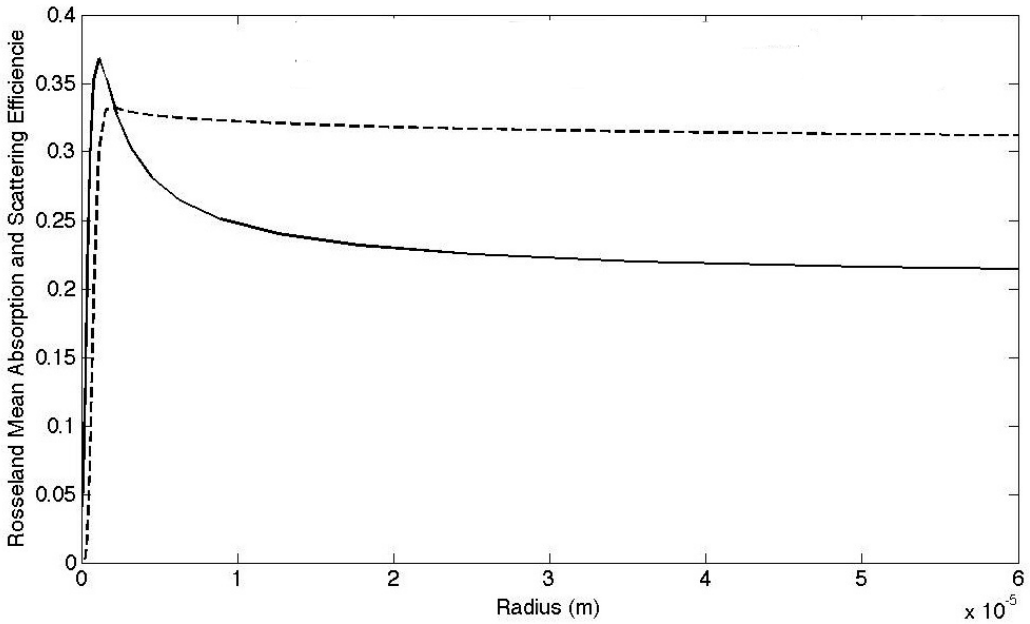

Figure 3.3. Variation of Rosseland mean absorption (solid line) and scattering (dashed line) efficiencies with coal particle radius.

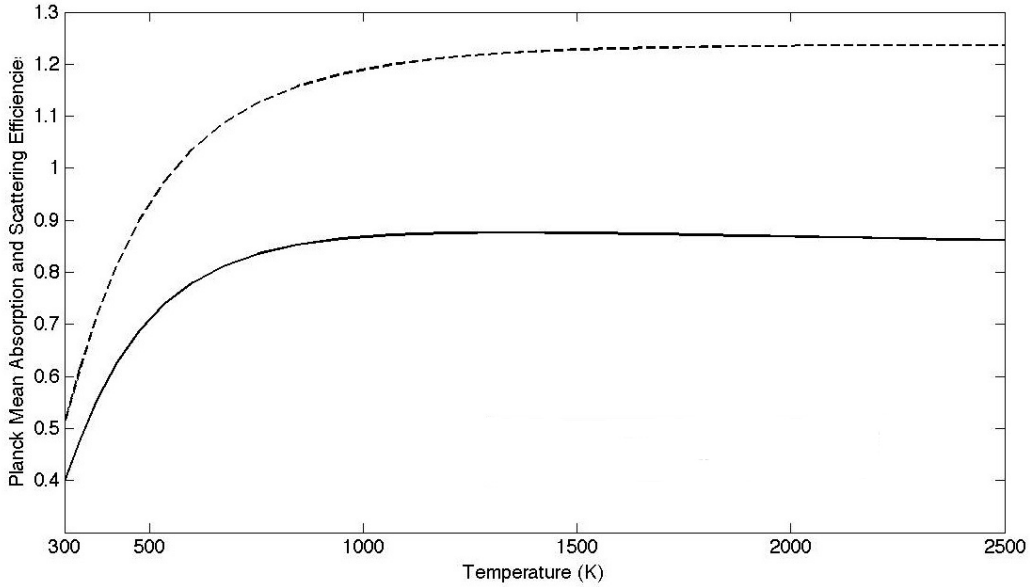

Figure 3.4. Variation of Planck mean absorption (solid line) and scattering (dashed line) efficiencies with coal particle temperature ($r = 25\mu m$).

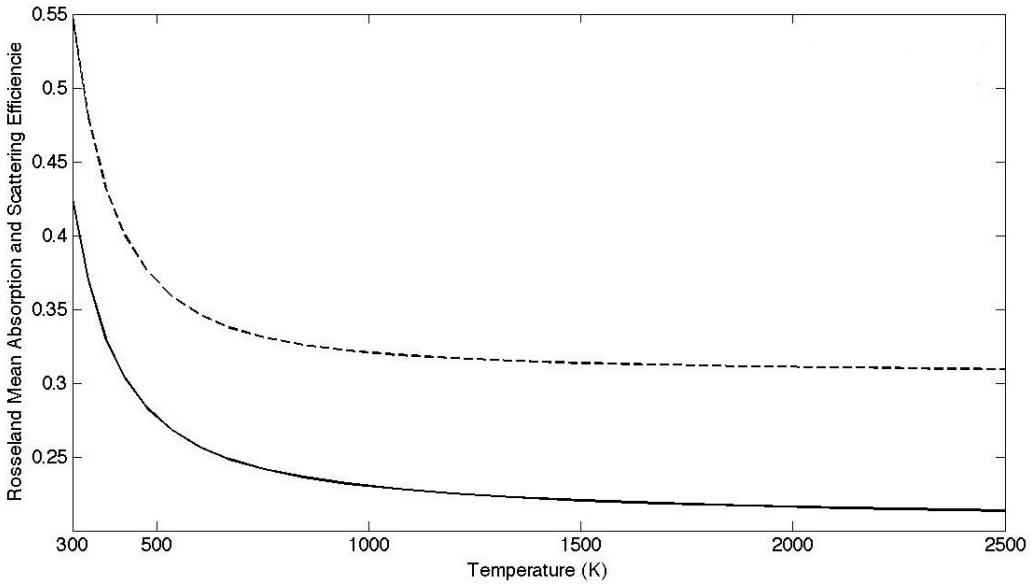

Figure 3.5. Variation of Rosseland mean absorption (solid line) and scattering (dashed line) efficiencies with coal particle temperature ($r = 25\mu m$).

Thus, if total (i.e., spectrally integrated) properties are desired, equations (3.7), (3.8), and (3.9) are integrated to give the Planck mean coefficients

$$\sigma_{s,P} = \pi a^2 N_T Q_{sca,P}, \tag{3.14}$$

$$\kappa_P = \pi a^2 N_T Q_{abs,P}, \tag{3.15}$$

$$\beta_P = \pi a^2 N_T Q_{ext,P}, \tag{3.16}$$

and the Rosseland mean coefficients

$$\sigma_{s,R} = \pi a^2 N_T Q_{sca,R}, \tag{3.17}$$

$$\kappa_R = \pi a^2 N_T Q_{abs,R}, \tag{3.18}$$

$$\beta_R = \pi a^2 N_T Q_{ext,R}. \tag{3.19}$$

The particle diameter and temperature are known from the combustion model. The Planck and Rosseland mean absorption and scattering efficiencies are calculated from the spectral efficiencies found from Mie theory. The mean efficiencies are calculated, tabulated, and stored as functions of particle diameter, temperature, and composition (refractive index), and are used to calculate radiative properties at a given cell location.

3.2.2 Clouds of Nonuniform Size Particles

When clouds of nonuniform size particles are considered, the contribution of each subset of particles of given size to the radiative coefficients must be added. For an array of radii a_j and corresponding number of particles n_j, the spectral scattering, absorption and extinctions coefficients are calculated by the following formulas

$$\sigma_{s\lambda} = \pi \sum_j n_j a_j^2 Q_{sca,j}, \tag{3.20}$$

$$\kappa_\lambda = \pi \sum_j n_j a_j^2 Q_{abs,j}, \tag{3.21}$$

$$\beta_\lambda = \pi \sum_j n_j a_j^2 Q_{ext,j}. \tag{3.22}$$

where the summation j, is over all particle sizes.

Similarly, the Planck and Rosseland mean coefficients are calculated

$$\sigma_{s,P} = \pi \sum_j n_j a_j^2 Q_{sca,P,j}, \tag{3.23}$$

$$\kappa_P = \pi \sum_j n_j a_j^2 Q_{abs,P,j}, \tag{3.24}$$

$$\beta_P = \pi \sum_j n_j a_j^2 Q_{ext,P,j}. \tag{3.25}$$

and

$$\sigma_{s,R} = \pi \sum_j n_j a_j^2 Q_{sca,R,j}, \tag{3.26}$$

$$\kappa_R = \pi \sum_j n_j a_j^2 Q_{abs,R,j}, \tag{3.27}$$

$$\beta_R = \pi \sum_j n_j a_j^2 Q_{ext,R,j}. \tag{3.28}$$

3.3 Rayleigh Scattering

Radiative scattering by spheres that are small compared to the wavelength was first described by Lord Rayleigh [21] long before the development of Mie's theory. However, results for small particles are most easily obtained by taking the appropriate limits in the general solution to Mie's equations.

If the scattering particles are extremely small, then the size parameter $x = {}^{2\pi a}/_{\lambda}$ becomes very small. Soot particles fall into the Rayleigh scattering regime. Soot particles, whose

diameters are often smaller than $10nm$, are irradiated by light of approximately $3\mu m$, resulting in $x \approx 0.01$.

In the limit of $x \to 0$,

$$S_2(\Theta) = S_1(\Theta)\cos(\Theta) = i\frac{m^2-1}{m^2+2}x^3\cos(\Theta),$$

that is, the amplitude function for one polarization is independent of scattering angle Θ. Substitution into equations (3.2) and (3.3) then gives the efficiency factors as

$$Q_{sca} = \frac{8}{3}\left|\frac{m^2-1}{m^2+2}\right|^2 x^4, \tag{3.29}$$

$$Q_{ext} = -4Im\left\{\frac{m^2-1}{m^2+2}\right\}x \approx Q_{abs}, \tag{3.30}$$

where the last equality in equation (3.30) is due to the fact that $x^4 \ll x$, so that scattering may be neglected as compared with absorption. The wavelength dependence of the scattering efficiency is [3]

$$Q_{sca} \propto \frac{1}{\lambda^4}.$$

The wavelength dependence of the absorption efficiency, on the other hand, is

$$Q_{abs} \propto \frac{1}{\lambda}.$$

The absorption coefficient for a cloud of nonuniform-size small particles with particle distribution function $n(a)$ is derived the following way [3]

$$\kappa_\lambda = \pi\int_0^\infty Q_{abs}a^2n(a)\,da = -4Im\left\{\frac{m^2-1}{m^2+2}\right\}\int_0^\infty \frac{2\pi a}{\lambda}\pi a^2n(a)\,da.$$

The integral in this equation may be related to the volume fraction f_v,

$$f_v = \int_0^\infty \frac{4}{3}\pi a^3n(a)\,da,$$

so that the absorption coefficient for small particles reduces to

$$\kappa_\lambda = -4Im\left\{\frac{m^2-1}{m^2+2}\right\}\frac{6\pi f_v}{\lambda},$$

or expanding the complex index of refraction, $m = n - ik$,

$$\kappa_\lambda = \frac{36\pi nk}{(n^2 - k^2 + 2)^2 + 4n^2k^2} \frac{f_v}{\lambda}. \tag{3.31}$$

Therefore, for particles small enough that Rayleigh scattering holds, the absorption coefficient does not depend on particle size distribution, but only on the total volume occupied by all particles (per unit system volume).

3.4 Numerical Algorithm

The software calculating the particle properties is written in C++. The code consists of two classes. The Mie Class, written by Orion Lawlor, calculates the wavelength-dependent Mie absorption and scattering efficiencies for a homogenous sphere of arbitrary size illuminated by coherent harmonic radiation [22]. The class ParticleRadCoeffs calculates and holds the spectrally resolved and effective absorption coefficients for particles. This class calculates, tabulates, and interpolates the following quantities

- $a_j^2 Q_{sca,j}$,
- $a_j^2 Q_{abs,j}$,
- $a_j^2 Q_{sca,P,j}$,
- $a_j^2 Q_{abs,P,j}$,
- $a_j^2 Q_{sca,R,j}$,
- $a_j^2 Q_{abs,R,j}$.

Given the particle size distribution function, the radiative coefficients for clouds of nonuniform size particles can be calculated from the appropriate tabulated quantities. The interpolation algorithm is bilinear:

$$k(x, y) = \alpha_0 + \alpha_1 x + \alpha_2 y + \alpha_3 xy,$$

where

$$\alpha_0 = (k(x_0, y_0)x_1y_1 - k(x_1, y_0)x_0y_1 - k(x_0, y_1)x_1y_0 + k(x_1, y_1)x_0y_0)/(dxdy),$$

$$\alpha_1 = ((k(x_1, y_0) - k(x_0, y_0))y_1 + (k(x_0, y_1) - k(x_1, y_1))y_0)/(dxdy),$$

$$\alpha_2 = ((k(x_0, y_1) - k(x_0, y_0))x_1 + (k(x_1, y_0) - k(x_1, y_1))x_0)/(dxdy),$$

$$\alpha_3 = (k(x_0, y_0) - k(x_1, y_0) - k(x_0, y_1) + k(x_1, y_1))/(dxdy).$$

The interpolation variables x and y are radius and wavelength for the spectral coefficients and temperature and radius for the mean coefficients, and the interpolation algorithm stores

the coefficients $\alpha_0, \ldots, \alpha_3$. The range of the particle radii is $1e^{-7}$ to $1e^{-4}$ m, and the range of the temperatures is 296 to 3000 K. The error due to interpolation in temperature and radius of the effective coefficients is calculated according to the formula

$$\epsilon = \max_{k_{mean}} \frac{|k_{interp} - k_{mean}|}{k_{mean}},$$

and plotted in Figure 3.6.

The mean absorption and scattering coefficients is estimated by calculating it at 10, 20, and 30 temperatures and 10, 20, and 30 radii. The interpolation is very sensitive to number of radii, due to the large range of radii we consider. The error in accuracy due to the number of temperatures is relatively small.

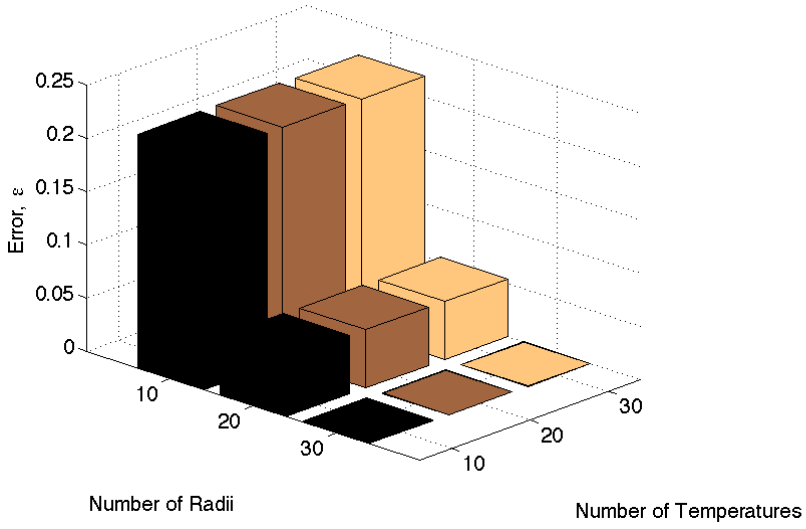

Figure 3.6. Error due to interpolation of the mean absorption and scattering coefficients in temperature and radius.

REFERENCES

[1] "ICSE simulation tools," *The Institute for Clean and Secure Energy.* [Online]. Available: http://www.ices.utah.edu

[2] L. Rothman, C. Rinsland, A. Goldman, S. Massie, D. Edwards, J. Flaud, A. Perrin, C. Camy-Peyret, V. Dana, J. Mandin, J. Schroeder, A. Mccann, R. Gamache, R. Wattson, K. Yoshino, K. Chance, K. Jucks, L. Brown, V. Nemtchinov, and P. Varanasi, "The HITRAN Molecular Spectroscopic Database and HAWKS (HITRAN Atmospheric Workstation): 1996 Edition," *Journal of Quantitative Spectroscopy and Radiative Transfer*, vol. 60, pp. 665–710, 1998.

[3] M. Modest, *Radiative Heat Transfer*, 2nd ed. Academic Press, 2003.

[4] G. Herzberg, *Molecular Spectra and Molecular Structure, Vol. II: Infrared and Raman Spectra of Polyatomic Molecules.* Princeton, NJ: Van Nostrand, 1945, vol. 2.

[5] C. Tien and J. Lienhard, *Statistical thermodynamics*, ser. Holt, Rinehart and Winston series in mechanical engineering. New York, NY: Holt, Rinehart, and Winston, 1971.

[6] M. Modest and H. Zhang, "The full-spectrum correlated-k distribution for thermal radiation from molecular gas-particulate mixtures," *ASME Journal of Heat Transfer*, vol. 124, no. 1, pp. 30–38, 2002.

[7] V. Solovjov and B. Webb, "Slw modeling of radiative transfer in multicomponent gas mixtures," *Journal of Quantitative Spectroscopy and Radiative Transfer*, vol. 65, pp. 655 – 672, 2000.

[8] M. Modest, "Narrow-band and full-spectrum k-distributions for radiative heat transfer - correlated-k vs. scaling approximation," *Journal of Quantitative Spectroscopy and Radiative Transfer*, vol. 76, no. 1, pp. 69 – 83, 2003.

[9] M. Denison and B. Webb, "The spectral line weighted-sum-of-gray-gases model - a review," in *Proceedings of the First International Symposium on Radiation Transfer Journal of Quantitative Spectroscopy and Radiative Transfer*, M. P. Menguc, Ed. Begell House, 1996, pp. 193 – 208.

[10] J. Taine and A. Soufiani, "Gas ir radiative properties: From spectroscopic data to approximate models," in *Advances in Heat Transfer*, vol. 33. New York: Academic Press, 1999, pp. 295 – 414.

[11] R. Patch, "Effective absorption coefficients for radiative energy transport in nongray, nonscattering gases," *Journal of Quantitative Spectroscopy and Radiative Transfer*, vol. 7, no. 4, pp. 611 – 637, 1967.

[12] Y. Babikov, "HITRAN and HITEMP databases on the web." [Online]. Available: http://hitran.iao.ru/gasmixture/spectr

[13] C. Tien and B. Drolen, "Thermal radiation in particulate media with dependent and independent scattering," in *Annual Review of Numerical Fluid Mechanics and Heat Transfer*, ser. 1, 1987, pp. 1–32.

[14] H. Hulst and H. van de Hulst, *Light Scattering by Small Particles*, ser. Structure of Matter Series. Dover Publications, 1957.

[15] H. Hottel, A. Sarofim, W. Dalzell, and I. Vasalos, "Optical properties of coatings. effect of pigment concentration." *AIAA Journal*, vol. 9, pp. 1895 – 1898, 1971.

[16] M. Brewster and C. Tien, "Radiative transfer in packed/fluidized beds: Dependent versus independent scattering," *ASME Journal of Heat Transfer*, vol. 104, pp. 573 – 579, 1982.

[17] J. Cartigny, Y. Yamada, and C. Tien, "Radiative transfer with dependent scattering by particles, part 1: Theoretical investigation," *ASME Journal of Heat Transfer*, vol. 108, pp. 608 – 613, 1986.

[18] B. Drolen and C. Tien, "Independent and dependent scattering in packed-sphere systems," *Journal of Thermophysics and Heat Transfer*, vol. 1, pp. 63 – 68, 1987.

[19] Y. Yamada, J. Cartigny, and C. Tien, "Radiative transfer with dependent scattering by particles, part 2: Experimental investigation," *ASME Journal of Heat Transfer*, vol. 108, pp. 614 – 618, 1986.

[20] B. Adams, "Computational evaluation of mechanisms affecting radiation in gas and coal-fired industrial furnaces," Ph.D. dissertation, University of Utah, 1993.

[21] L. Rayleigh, "On the light from the sky, its polarization and colour," *Philos. Mag.*, vol. 41, pp. 107 – 120, 274 – 279, 1871.

[22] O. Lawlor, "Mie Spherical Scattering Algorithm: C++ Implementation," 2011. [Online]. Available: http://www.scattport.org/index.php/programs-menu/mie-type-codes-menu/268-scatter-mie